On the mechanism of theta capillary nanoelectrospray ionization for the formation of highly charged protein ions directly from native solutions

Susannah L. Brown,[1] Muhammad A. Zenaidee,[2,†] Joseph A. Loo,[2] Rachel R. Ogorzalek Loo,[2] William A. Donald[1,*]

[1]School of Chemistry, University of New South Wales, Sydney 2052, Australia

[2]Department of Chemistry and Biochemistry, University of California Los Angeles, Los Angeles, California 90095, United States of America

[*]To whom correspondence should be addressed: w.donald@unsw.edu.au

ABSTRACT

Theta capillary nanoelectrospray ionization (θ-nanoESI) can be used to 'supercharge' protein ions directly from solution for detection by mass spectrometry (MS). In native top-down MS, the extent of protein charging is low. Given that ions with more charge fragment more readily, increasing charge can enhance the extent of sequence information obtained by top-down MS. For θ-nanoESI, dual-channelled nanoESI emitters are used to mix two solutions in low to sub-μs prior to MS. The mechanism for θ-nanoESI mixing has been reported to primarily occur: (i) in a single shared Taylor cone and in the droplets formed from the Taylor cone, or (ii) by the fusion of droplets formed from two separate Taylor cones. Using θ-nanoESI-ion mobility-MS, native protein solutions were rapidly mixed with denaturing supercharging solutions to form protein ions in significantly higher charge states and with more elongated structures than those formed by pre-mixing the solutions prior to nanoESI-MS. If θ-nanoESI mixing occurred in the Taylor cone and in the droplets resulting from the single Taylor cone, then the extent of protein charging and unfolding should be comparable or less than that obtained by pre-mixing solutions. Thus, these data are consistent with mixing occurring via droplet fusion rather than in the Taylor cone prior to ESI droplet formation. These data also suggest that highly charged protein ions can be formed by the near complete mixing of each solution. The presence of supercharging additives in pre-mixed solutions can suppress volatile electrolyte evaporation, limiting the extent of protein charging compared to when the additive is delivered via one channel of a θ-nanoESI emitter. In θ-nanoESI, the formation of two Taylor cones can presumably result in substantial electrolyte evaporation from the ESI droplets containing native-like proteins prior to droplet fusion, thereby enhancing ion charging.

TABLE OF CONTENTS GRAPHIC

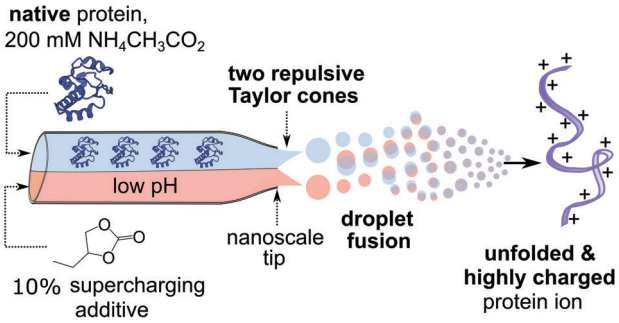

Top-down mass spectrometry (MS)-based proteomics is rapidly becoming a central method for the characterization of intact proteins and protein complexes.[1] Electrospray ionization (ESI) is renowned for its ability to transfer intact proteins and protein complexes from the solution to the gas phase.[2] Multiple charging is beneficial in tandem mass spectrometry (MS/MS) measurements for enhancing sequence information in charge-state dependent fragmentation methods (*e.g.,* electron capture dissociation, electron transfer dissociation, and ultraviolet photodissociation at lower pressures),[3–6] and signal increases proportionally with charge state for charge sensitive detection (*e.g.,* FT-ICR, Orbitrap and charge detection MS[7]). Protein ions formed from denaturing solutions typically have higher and broader charge state distributions than those formed from native-like solutions because the unfolded conformations have higher surface areas and thus, more protonation sites can be accommodated.[8] In contrast, protein ions generated from native-like solutions can be compact and more closely represent their native-like conformations. Retaining the native-like structures of proteins in the gas-phase is important for obtaining accurate information regarding non-covalent complexes (*e.g.,* ligand binding affinities and locations, stoichiometry, and assembly dynamics).[9,10] In methods that use isotopic or reactive labelling and whole protein mass spectrometry to probe solution-phase protein structure (*e.g.,* top-down hydrogen-deuterium exchange[11–14] and fast photochemical oxidation of proteins[15,16]), it is often beneficial to maximize protein ion charging, and retaining native-like structures after ion formation is not necessarily required. Enhancing charge states is also beneficial in limited charge reduction experiments for the analysis of heterogeneous, high mass complexes in native mass spectrometry.[17]

Several methods have been developed to increase the charge states of protein ions formed from native solutions, collectively termed ‘native supercharging’. Native supercharging methods include: (i) doping small molecule additives with low vapor pressure

directly into native protein solutions in low concentrations (*e.g.*, *m*-nitrobenzyl alcohol[18–22] or sulfolane[19,23,24]), (ii) increasing the electric field between the ESI emitter and the MS entrance ("electrothermal supercharging"),[25] (iii) increasing the gas pressure in the ion source,[26] and (iv) dual channel ESI using theta capillaries for rapid mixing of the native and denaturing solutions during the ESI process.[27,28] For the latter method, the extent of protein ion charging can be increased by more than 100% compared to the alternative methods for common test proteins.[28]

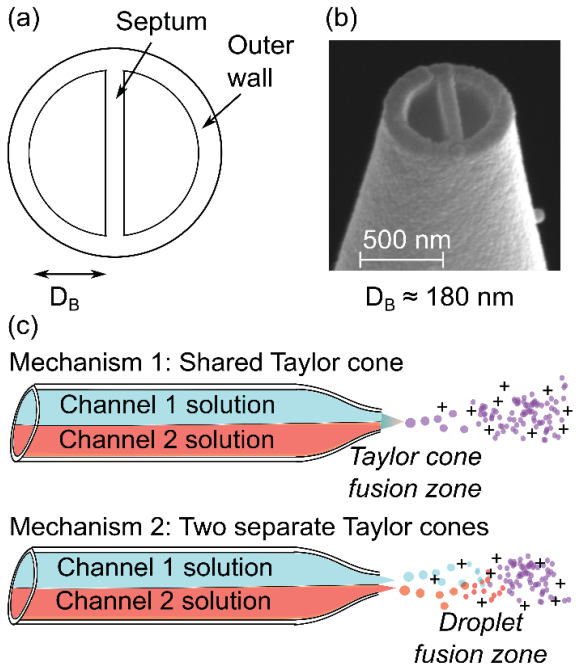

Figure 1. Theta nanoelectrospray ionization (θ-nanoESI) emitters and mechanisms. (a) Cross section of θ-nanoESI emitters. D_B represents the diameter of each channel perpendicular to the septum. (b) Representative scanning electron micrograph of the tip of the θ-nanoESI emitters used in this work where the diameter D_B is approximately 180 nm. (c) In mechanism 1, the two solutions mix in a shared Taylor cone and inside the resulting droplets. In mechanism 2, a separate Taylor cone forms from each channel and droplets undergo fusion to result in combined droplets containing a mixture of the two solutions.

Theta capillaries are nanoelectrospray ionization (nanoESI) emitters that are divided into two channels by a glass septum[29,30] which can be used to rapidly mix two solutions during

ESI prior to MS analysis (**Figure 1a, b**). The mixing process can occur within microseconds to sub-microseconds.[29,31] Theta nanoESI (θ-nanoESI) has been used to measure rapid HDX rates in liquid droplets[32,33] (*e.g.,* 3660 s^{-1} for formation of $–NH_2D^+$ from $–NH_3^+$),[32] to probe protein folding/unfolding,[31,34] and to observe short-lived reaction intermediates.[30] In native supercharging via θ-nanoESI, one channel of the theta capillary is loaded with a native protein solution (in ammonium acetate) and the other channel can be loaded with a denaturing solution containing a supercharging agent, such as a cyclic alkyl carbonate supercharging additive (*e.g.,* 4-vinyl-1,3-dioxolan-2-one or 1,2-butylene carbonate).[28] The mixing of the two solutions during the ESI process can result in the formation of protein ions in comparable charge states as those formed directly from a denaturing supercharging solution. The rapid timescale of mixing and high protein ion charge states that can be formed should be particularly useful for probing solution-phase structure by hydrogen-deuterium exchange MS.[13] However, the mechanism of solution mixing in θ-nanoESI has been the subject of some controversy in the literature.

Since the first use of theta capillaries in mass spectrometry experiments,[30] two primary mechanisms have been proposed for solution mixing. The more commonly invoked mechanism for θ-nanoESI is that the two solutions are mixed within a single Taylor cone and in the resulting droplets formed from this Taylor cone (**Figure 1c**).[27,29,30] This 'shared Taylor cone' mechanism has been suggested for tips ranging in size from ~600[29] to 4000[27] nm per channel (D_B in **Figure 1a**). Based on the use of confocal microscopy to probe the mixing of two dyes rhodamine B and fluorescein in two separate channels of theta capillaries (D_B of ~2000 nm; **Figure 1a**), Derrick and co-workers[30] reported that a single Taylor cone was visible in early θ-nanoESI experiments. More recently, Derrick and co-workers[35] proposed that mixing could also occur via the coalescence of charged droplets after their formation, although high speed

microscopy data of non-tapered θ-nESI emitters with large orifices (D_B of ~300 μm) supported the single Taylor cone mechanism.

In 2017, Zare and coworkers[32] queried the shared Taylor cone mechanism that mixing occurred primarily in the Taylor cone and in the droplets resulting from a single Taylor cone. Micro-particle image velocimetry was used to visualize the Taylor cone and spray region for theta capillary tips with channels that were ~2000 nm wide (D_B of ~2000 nm; **Figure 1a**). Microscopy images revealed a separate Taylor cone-jet originating from each theta capillary channel with the two plumes repulsing each other owing to Coulombic repulsion. At ~200 μm from the exit of the theta tip, droplets from the two sprays began to fuse. The authors suggested that the – physically unexpected – fusion of repulsive droplets resulted from inertial mixing, in which frequent and highly energetic collisions between charged droplets can overcome their Coulombic repulsion (**Figure 1c**). Any mixing in the Taylor cone was estimated to be more than 10^5 times lower than via droplet fusion based on a computational fluid dynamics model.

In this work, the mechanism of θ-nanoESI is investigated for emitter tips in which the orifice sizes are < 200 nm wide (**Figure 1b**). Using ion mobility MS, we demonstrate that rapid mixing of native-like protein (containing ammonium acetate) and denaturing supercharging solutions using θ-nanoESI results in protein ions that are significantly more unfolded than protein ions formed when the two solutions are mixed prior to ESI. Furthermore, protein ions formed from θ-nanoESI of native and denaturing supercharging solutions are comparable to those formed directly from denaturing supercharging solutions (without ammonium acetate) in terms of charge and conformations. These results are more consistent with the mixing of the native and denaturing supercharging solutions occurring via separate Taylor cones and subsequent droplet fusion.

METHODS

Experiments were performed on a Synapt G2-Si quadrupole-time-of-flight (Q-ToF) mass spectrometer with a travelling wave (T-wave) ion mobility spectrometry (TWIMS) cell (Waters Corp.; Milford, MA, USA), and a NanoLockSpray nanoelectrospray ionization source, in which the nanoelectrospray ionization emitter is positioned perpendicular to the sample cone at the MS inlet. All solutions were electrosprayed at a flow rate of ~20 nL/min by applying 0.9-1.2 kV to the emitter tip. The source temperature was set to 80-100ºC. For each solution investigated, 100 mass spectra were collected and averaged. All mass spectra were externally calibrated using caesium iodide. Au/Pd coated borosilicate single channel nanoelectrospray ionization emitters were purchased from Thermo Fisher Scientific (1.2 mm o.d., ~1 μm i.d.; San Jose, CA, USA). Dual channel nanoelectrospray ionization emitters were pulled from borosilicate capillaries (1.5 mm o.d., theta capillary, Harvard Apparatus, USA) to a tip inner orifice diameter of ~180 nm per channel perpendicular to the dividing septum (**Figure 1**) using a microcapillary puller (P-97, Sutter Instruments) and sputter-coated with a thin layer of Au/Pd (1:1 mol ratio) for 20 s (Scancoat Six, Edwards, UK). The tip dimensions were measured by scanning electron microscopy imaging (FEI Nova NanoSEM 450 FE-SEM, Thermo Fisher Scientific). All materials were purchased from commercial sources. Refer to Supporting Information for details.

MassLynx (Waters) was used to process mass spectra and arrival time distributions. Mean and error values for average charge states and collision cross sections were calculated from triplicate measurements using a different emitter for each measurement. Errors are reported as one standard deviation. To calculate collision cross sections (CCS), calibration curves were created for converting measured arrival times to CCS values. TWIMS arrival times for cytochrome *c* (13+ to 19+) and apo-myoglobin (15+ to 24+) ions formed from denaturing

solutions of 10 μM protein in 48.25/48.25/3.5 water/methanol/acetic acid (%/% v/v), were first corrected for *m*/*z* dependent flight times, according to,

$$t_{\mathrm{d}'} = t_{\mathrm{d}} - 0.001 \times t_{EDC} \times m/z^{0.5}$$

where $t_{\mathrm{d}'}$ is the corrected arrival time, t_{d} is the measured arrival time, and t_{EDC} is the enhanced duty cycle delay coefficient which is 1.30 ms for the Synapt G2-Si. The measured arrival time values used were the mean of Gaussian distributions fitted using GraphPad Prism 9.0.0 for Windows (GraphPad Software, San Diego, California USA). The average of three separate measurements was used. Calibrant CCS values[36] were corrected for charge and reduced mass according to:

$$\mathrm{CCS}' = \frac{\mathrm{CCS}}{z \times \left(\frac{1}{\mathrm{MW(protein)}} + \frac{1}{\mathrm{MW(N_2)}}\right)^{0.5}}$$

where CCS′ is the corrected CCS value, CCS is the literature CCS value,[36] z is the charge, MW(protein) is the molecular weight of the protein, MW(N_2) is the molecular weight of the drift gas, N_2. The natural logarithm of CCS′ and $t_{\mathrm{d}'}$ were used in the calibration curves. The resulting calibration curves had R^2 values of 0.9895 (cyt *c*) and 0.9958 (apo-myoglobin). To estimate CCS values corresponding to the native, alpha-helical, and near-linear states of cytochrome *c*, apo-myoglobin, and carbonic anhydrase II in nitrogen, the linear calibration curve obtained by Williams and coworkers[37] for converting helium cross sections to nitrogen cross sections was used. Cross sections in helium were calculated using the exact hard-spheres scattering model[38] simulations for cytochrome *c* and apo-myoglobin by Jarrold and coworkers,[39] and converted to nitrogen values using the linear conversion:

$$\mathrm{CCS_{N_2}} = \mathrm{CCS_{He}} \times 1.2806 + 0.2432$$

To estimate the CCS values for the three states of carbonic anhydrase II, the CCS values for cytochrome *c* and apo-myoglobin were extrapolated based on the relative number of amino acid residues. The CCS per amino acid residue is linearly proportional to the charge per amino

acid residue. Specifically for helium, the native state CCS values increase by ~12 $Å^2$ $residue^{-1}$, the alpha-helical state CCS values increase by ~22 $Å^2$ $residue^{-1}$, and the near-linear state CCS values increase by ~33 $Å^2$ $residue^{-1}$.[39]

RESULTS AND DISCUSSION

Formation of highly charged protein ions from native solutions using theta nanoelectrospray ionization emitters. Protonated ions of cytochrome *c*, apo-myoglobin, and carbonic anhydrase II were formed from either: (i) a single channel nanoESI capillary containing the protein in a denaturing supercharging solution of 45.75/45.75/5/3.5 water/methanol/1,2-butylene carbonate (BC)/acetic acid (%/% v/v) (conventional nanoESI), or (ii) a theta capillary in which one channel contained a native protein solution (pH ~7 in 200 mM ammonium acetate) and the second channel contained a solution of 41.5/41.5/10/7 water/methanol/BC/acetic acid (%/% v/v) (θ-nanoESI) (**Figure 2**). BC is added to significantly increase the protein ion charge states (**Figure S1**), as also shown in previous studies.[40] The extent of charging for cytochrome *c*, apo-myoglobin and carbonic anhydrase II formed from native-like solutions from one channel of a theta capillary was relatively low and consistent with that expected for native MS (**Figure S2**). Since protein ion charging in ESI is highly dependent on the applied spray voltage and the distance from the tip to the inlet, these parameters were optimized using cytochrome *c* to ensure maximum charging (**Figure S3**). The orientation of the dividing septum of the theta tip to the inlet of the mass spectrometer did not strongly affect protein ion charging or arrival time distributions (**Figure S4**). In addition, the use of a single channel of a θ-nanoESI emitter compared to the use of a conventional emitter of a similar orifice size does not generally affect the observed protein ion charge state distributions (see below and **Figure S5**).

For all three proteins studied, similar ion charge state distributions were obtained from both conventional nanoESI of a denaturing supercharging protein solution, and θ-nanoESI

mixing of a native-like protein solution with a denaturing supercharging solution (**Figure 2 a-f**). For example, when formed by conventional nanoESI (or θ-nanoESI) the most abundant charge state of cytochrome *c* ions (MACS) was 21+ (21+), the highest observed charge state (HOCS) was 23+ (23+) and the average charge state (ACS) was 19.8 ± 0.1 (19.1 ± 0.6) (**Figure 2a, d**). Similar results were obtained for apo-myoglobin (**Figure 2b, e**) and carbonic anhydrase II (**Figure 2c, f**). In a previous report[28] in which θ-nanoESI was used for native protein supercharging, protein ion charge states were higher than those observed here. For example, the average charge state reported for cytochrome *c* was 23.1 ± 0.1 compared to 19.1 ± 0.6 in **Figure 2d**.[28] These data are consistent with the higher charging obtained by using an instrument with a capillary-skimmer ion source interface[3,40–42] compared to that obtained using a Z-spray ion source interface (of the Synapt G2-Si instrument)[37] for standard protein ions formed from denaturing, cyclic alkyl carbonate supercharging solutions. These data further demonstrate that theta capillary nanoESI emitters can be used to form protein ions directly from native solutions in comparable charge states as those formed from denaturing solutions by conventional nanoESI.

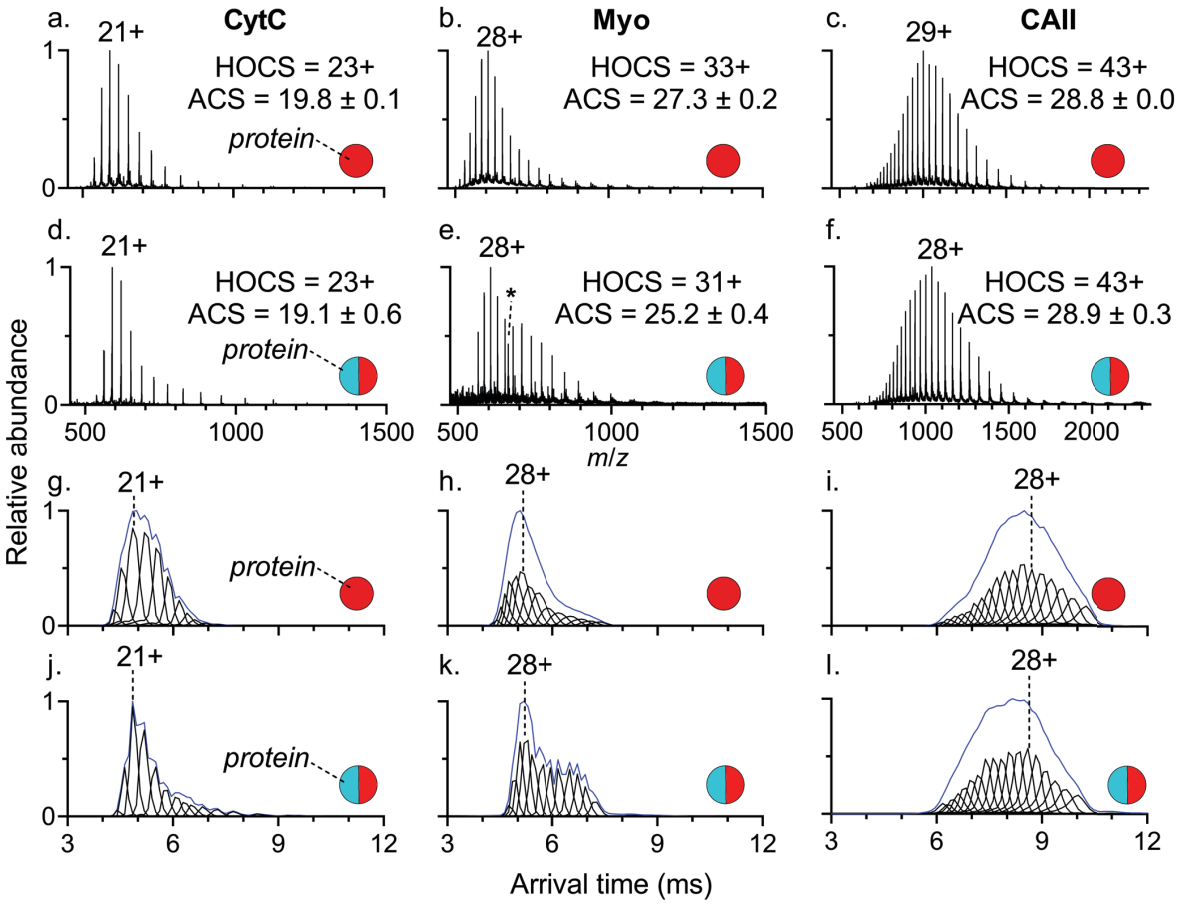

Figure 2. Protein ions formed by theta capillary 'native supercharging' have charge states and arrival time distributions comparable to protein ions formed directly from denaturing-supercharging solutions. Representative (a-f) mass spectra and (g-l) TWIMS arrival time distributions for individual charge states (black) and summed (blue) for (a, d, g, j) cytochrome *c*, (b, e, h, k) apo-myoglobin, and (c, f, i, l) carbonic anhydrase II ions formed from either (a-c, g-i) a single channel nanoESI capillary with a denaturing supercharging solution containing 10 μM protein with 45.75/45.75/5/3.5 water/methanol/1,2-butylene carbonate/acetic acid (%/% v/v), or (d-f, j-l) a theta capillary with one channel containing 10 μM protein in 200 mM ammonium acetate (pH ~7) and the other channel a solution of 41.5/41.5/10/7 (%/% v/v) water/methanol/1,2-butylene carbonate/acetic acid. The most abundant charge state, highest observed charge state (HOCS) and average charge state (ACS) are indicated. The asterisk indicates a peak corresponding to a chemical contaminant.

To compare the conformations of the highly charged protein ions formed by θ-nanoESI with those formed using conventional nanoESI, TWIMS was used. For all three proteins studied, similar arrival time distributions for the entire charge state envelopes were obtained from both conventional nanoESI of a denaturing supercharging protein solution, and θ-nanoESI mixing of a native-like protein solution and a denaturing supercharging solution (**Figure 2**). For all three proteins, the maxima of the arrival time distributions are consistent for ions formed by conventional nanoESI or θ-nanoESI. The width of the arrival time distributions for apo-myoglobin formed from θ-nanoESI is wider compared to conventional nanoESI (**Figure 2h, k**) and mirrors the trends in widths for the corresponding charge state distributions. This wider arrival time distribution could be explained by slightly less unfolding of the protein ion on the timescale of solution mixing, ion formation, transfer and detection. However, the overall similarity between the arrival time distributions for protein ions formed by conventional nanoESI compared to θ-nanoESI indicates that the extent of elongation of the protein ions formed by these two methods are largely comparable. Furthermore, since the protein ions formed from denaturing supercharging solutions should be largely unfolded, these data indicate that the protein ions formed by θ-nanoESI from native solutions can unfold during the electrospray process.

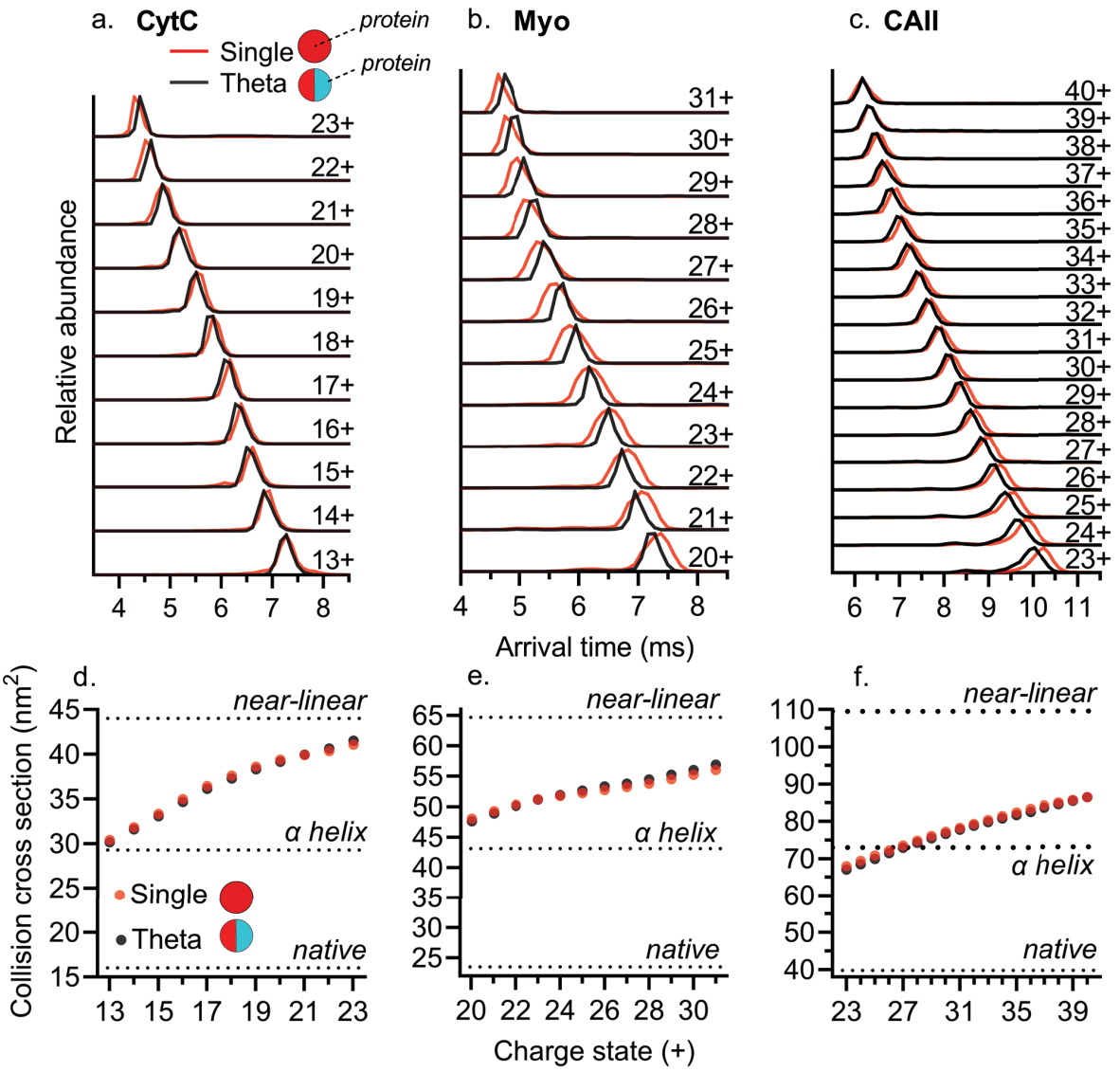

Figure 3. Theta capillary native supercharging results in unfolded protein ions with similar conformations to protein ions formed directly from denaturing-supercharging solutions. (a-c) TWIMS arrival time profiles of individual charge states, and (d-f) collision cross sections (CCS) as a function of charge state, when formed from either a single channel nanoESI capillary with a denaturing supercharging solution containing 10 μM (a,d) cytochrome c, (b,e) apo-myoglobin or (c,f) carbonic anhydrase II with 45.75/45.75/5/3.5 water/methanol/1,2-butylene carbonate/acetic acid (%/% v/v) (red plots) or a theta capillary with one channel containing 10 μM protein in 200 mM ammonium acetate (pH ~7) and the other channel a solution of 41.5/41.5/10/7 water/methanol/1,2-butylene carbonate/acetic acid

(%/% v/v) (black plots). Dotted lines correspond to the approximate collision cross sections of the protein ions in their native, α-helical and near-linear states.[33,35] Error bars correspond to the standard deviation of triplicate measurements and are not visible (< 0.6%).

To investigate the extent of protein unfolding during the ionization process in θ-nanoESI, the arrival time distributions and collision cross sections (CCS) of individual charge states of cytochrome *c*, apo-myoglobin, and carbonic anhydrase II formed from θ-nanoESI mixing were compared to those formed directly by conventional nanoESI of denaturing supercharging protein solutions (**Figure 3**). Interestingly, for all three proteins, individual charge states had similar arrival time distributions (**Figure 3a-c**) and CCSs (**Figure 3 d-f**) under both nanoESI conditions (differences in CCS <1.5%). As expected, the arrival times for the ions of the three proteins decrease with increasing charge state and decreasing mass (**Figure 3a-c**). The similarity in arrival time distributions and CCS for ions formed by conventional nanoESI and θ-nanoESI further indicate that the conformation of ions formed from native solutions by θ-nanoESI mixing with denaturing supercharging solutions are directly comparable to those formed from denaturing conditions in conventional nanoESI.

The extent of unfolding in θ-nanoESI was further investigated by comparing the experimental CCS values to theoretical CCS values of near-linear, completely alpha helical, and native conformations for each of the three proteins (as calculated previously, see **Experimental**),[39] which are shown in **Figure 3d-f**. These data indicate that the cytochrome *c* ions (13 to 23+) formed from θ-nanoESI mixing and conventional nanoESI are both largely unfolded, with CCS values that are between those corresponding to alpha helical (~30 nm^2) and near-linear (~44 nm^2) conformations. Similarly for apo-myoglobin ions (20+ to 32+), the CCS values indicate largely unfolded conformations formed from both θ-nanoESI and conventional nanoESI. For carbonic anhydrase II ions (23+ to 40+), CCS values also indicate a degree of protein unfolding, with values comparable to or slightly larger than completely

alpha helical. These results demonstrate that highly charged protein ions formed from native solutions by θ-nanoESI mixing can be more elongated than 'perfect' alpha helices and can approach conformations with similar CCS values as near-linear conformations. The charge and conformation of these highly charged protein ions formed from θ-nanoESI mixing appear to be directly comparable in charge and conformations to those formed from denaturing solutions. That is, the rapid mixing during the ionization process of native and denaturing supercharging solutions via θ-nanoESI results in protein ions which are both highly charged and unfolded.

Formation of protein ions via θ-nanoESI mixing vs. in-solution mixing. To compare protein ion formation between mixing solutions via θ-nanoESI and mixing in-solution prior to nanoESI, ions of cytochrome *c*, apo-myoglobin and carbonic anhydrase II were formed by θ-nanoESI mixing of a native protein solution (200 mM ammonium acetate, ~pH 7) and a denaturing supercharging solution containing 41.5/41.5/10/7 water/methanol/BC/acetic acid (%/% v/v), or from one or both channels of a θ-nanoESI capillary containing a 1:1 (v:v) mixture of the native protein and denaturing supercharging solutions. This latter approach is referred to as "in-solution mixing" or "pre-mixing" and the former as "θ-nanoESI". For cytochrome *c*, the pre-mixed solution (1:1 mix of native protein solution and denaturing supercharging solution) was left to equilibrate overnight at 4ºC and was electrosprayed from one or two channels of a theta capillary. The overnight incubation was performed to allow sufficient time for protein structural changes resulting from mixing to equilibrate. The resulting spectra were compared to θ-nanoESI spectra collected immediately prior (**Figure S6**). Cytochrome *c* ions formed after in-solution mixing had significantly lower charge states compared to those formed by θ-nanoESI. Moreover, the charge state distributions were not affected by whether the pre-mixed solution was sprayed from one channel (**Figure S6a**) or both channels (**Figure S6c**) of the theta capillary. That is, θ-nanoESI mixing of the native protein and denaturing supercharging solutions resulted in a charge state distribution with an ACS of 19.4 ± 0.1, which was

significantly higher than those ions formed after the pre-mixed solution was electrosprayed from one (15.6 ± 0.1) or both (15.5 ± 0.1) channels of a theta capillary, respectively (**Figure S6a, c, e**). We also compared the effects of electrospraying a pre-mixed solution (pre-mixed just prior to MS measurement) from one side of a theta capillary to a conventional single channel nanoESI capillary and observed no significant differences, indicating that the tip geometry itself does not affect the extent of protein ion charging and unfolding (**Figure S5**). For apo-myoglobin and carbonic anhydrase II (**Figure S7**), the pre-mixing was performed just prior to nanoESI because overnight incubation of the native protein and denaturing supercharging solutions led to some protein degradation. Similarly to cytochrome *c*, the mass spectra of apo-myoglobin and carbonic anhydrase II for in-solution mixing prior to nanoESI compared to θ-nanoESI were remarkably different (**Figure S7**). For both proteins, nanoESI of pre-mixed solutions resulted in significantly lower ion charging compared to θ-nanoESI mixing. Furthermore, for all three proteins studied, the TWIMS arrival time distributions for the entire charge state distributions formed after in-solution mixing (**Figures S6b, d and S7e, f**) were broader and shifted to longer times than those formed using θ-nanoESI mixing (**Figures S6f and S7g, h**). Broader arrival time distributions indicate that the protein ions formed by in-solution mixing generally exhibited a larger range of conformations compared to those formed by θ-nanoESI mixing. The longer arrival times reflect the lower charge states observed from in-solution mixing as compared to θ-nanoESI mixing. These data indicate that rapid mixing of native protein solutions and denaturing solutions by θ-nanoESI during the electrospray process can result in significantly increased protein charging and conformational differences compared to when the solutions are mixed prior to nanoESI.

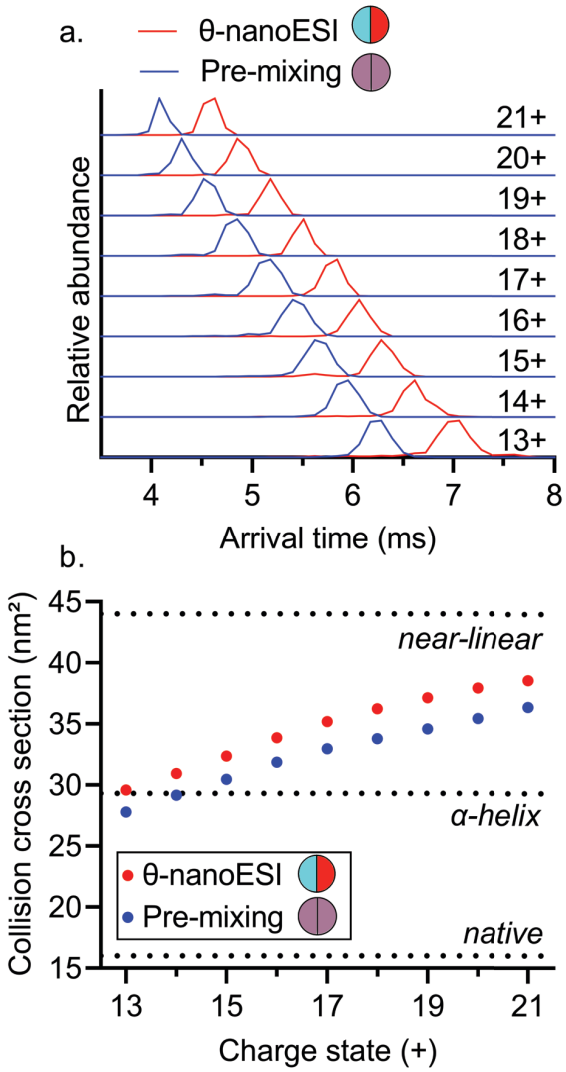

Figure 4. θ-nanoESI mixing of native cytochrome *c* solutions and denaturing, supercharging solutions results in ions with larger collision cross sections than those formed after pre-mixing. (a) TWIMS arrival time distributions of individual charge states of cytochrome *c* formed from either theta nanoESI mixing (red) or pre-mixing (blue) of a 10 μM cytochrome *c* solution in 200 mM ammonium acetate (~pH 7) with a solution of 10/7/41.5/41.5 (%/% V/V) butylene carbonate/acetic acid/methanol/water. For pre-mixing, the solution was incubated overnight to reach equilibrium. The equilibrated mixture was loaded into both channels of a theta capillary. (b) Collision cross sections (CCS) as a function of charge state for θ-nanoESI mixing or pre-mixing where both channels were loaded with the equilibrated solution. Dotted lines correspond to the approximate collision cross sections of the protein ions

in their native, α-helical and near-linear states.[37,39] Error bars correspond to the standard deviation of triplicate measurements and are not visible (< 0.8%).

The extent of unfolding of protein ions formed by θ-nanoESI mixing or in-solution mixing was examined by comparing the TWIMS arrival time distributions and collision cross sections of equivalent charge states of cytochrome *c* (**Figure 4**). For in-solution mixing, the mixture was loaded into both channels of a θ-nanoESI emitter. Dramatic differences in ion arrival times and CCS values were observed when the ions were formed from θ-nanoESI (red data lines and points in **Figure 4**) compared to in-solution mixing prior to conventional nanoESI (blue data lines and points in **Figure 4**). The CCS values obtained for protein ions formed by θ-nanoESI in **Figure 4b** and **3d** were within an average of 2.6% of each other across nine charge states, even though these data were obtained on two different days under conditions that were optimised for either denaturing supercharging solutions (**Figure 3d**) or nanoESI of pre-mixed native protein and denaturing solutions (**Figure 4d**). Cytochrome *c* ions formed from θ-nanoESI had longer arrival times (between ~0.5 to 0.7 ms longer) than the equivalent charge states formed from in-solution mixing (**Figure 4d**). Furthermore, cytochrome *c* ions formed from θ-nanoESI mixing had 6-7% larger CCS than the corresponding ions formed after in-solution mixing (**Figure 4d**). These differences in TWIMS arrival times and CCS values indicate that ions formed from θ-nanoESI mixing were significantly more unfolded than those formed after in-solution mixing prior to nanoESI. These results are surprising because the compositions of the two solutions are identical, and thus the protein ion charging and conformations are strongly dependent on whether the two solutions are mixed prior to ESI or during the ESI process. Furthermore, the timescale of mixing in θ-nanoESI is significantly faster (sub to low μs) than in-solution pre-mixing (minutes to hours prior to nanoESI), so it would be expected that θ-nanoESI mixing would result in similar or lower protein charge states and similar or less unfolded conformations compared to pre-mixing prior to nanoESI. Thus,

these results suggest that the process of ion formation differ for mixing via θ-nanoESI compared to nanoESI after pre-mixing of the same solutions. Alternatively, the final droplet compositions from which the protein ions are emitted may differ for θ-nanoESI compared to nanoESI of the pre-mixed solutions.

Charge-manipulated ions (supercharged or charge-reduced) may differ subtly from equally charged ions produced directly by ESI.[43] One possibility is that supercharging additives such as BC may reduce the number of opposing charges present in electrosprayed proteins (*i.e.,* reduce aspartate and glutamate anionic sites in zwitterionic protein ions). Higher additive concentrations could exert a larger effect. As protein ions are electrohydrodynamically emitted from droplets,[43] higher BC concentrations in fusion-derived droplets (due to rapid methanol/acetic acid evaporation) could yield ions with fewer opposing charges (and, thus, fewer restraining ion pairs) than the protein ions released from pre-mixed droplets. Hence, more deformable cytochrome *c* ions from fusion-derived droplets could lead to larger CCSs than those of identically charged ions from pre-mixed solutions.

The mechanism of theta nanoelectrospray ionization. Two distinct mechanisms for θ-nanoESI have been reported in the literature (**Figure 1c**). In the two Taylor cone mechanism, solution mixing of the two solutions occurs by fusion of charged droplets derived from each theta capillary channel Taylor cone.[32] In the shared Taylor cone mechanism, the two solutions combine in a single Taylor cone to form initial ESI droplets that are a mixture of both solutions. The latter mechanism is more commonly invoked in the literature[27,29,30] including for θ-nanoESI with small bore tips.[29] Based on results in the literature from high-speed microscopy,[32] ESI from larger bore theta emitters (D_B of 2000 nm) can result in the formation of two separate Taylor cones. However, the mechanism is less clear for narrower bore emitters.

The electrospray droplet composition just prior to the moment of ion formation can be considered in four key scenarios: (i, ii) θ-nanoESI of native protein solutions and denaturing

supercharging solutions via the two different mechanisms (shared Taylor cone or dual Taylor cones; **Figure 1c**), (iii) conventional nanoESI of denaturing supercharging protein solutions, and (iv) conventional nanoESI of pre-mixed native protein solutions and denaturing supercharging solutions. In all cases, after the solutions exit the tip of the emitters, a stream of charged droplets form and are accelerated down a pressure and potential gradient towards the MS entrance. During this process, volatile components of the charged droplets evaporate, decreasing the radius and increasing the charge density of the droplets. If the electrostatic repulsion on the droplet surface overcomes the droplet surface tension (*i.e.,* near the Rayleigh limit),[44–46] ESI droplets undergo fission to produce offspring droplets. Cycles of evaporation and fission can occur until fully desolvated gaseous ions are formed.

The extent of protein ion charging was significantly higher when using a standard denaturing supercharging solution (**Figure 2**) that did not contain ammonium acetate than for the pre-mixed solutions that contained ammonium acetate (**Figures S5 and S6**). The only key difference between these two solutions is the presence of 100 mM ammonium acetate in the pre-mixed solution. Thus, the use of ammonium acetate significantly decreased the extent of protein charging under these conditions. Ammonium acetate is often used in native mass spectrometry to reduce protein ion unfolding and salt adduction, and to increase solution conductivity and ionic strength.[44] ESI-generated droplets formed from the pre-mixed solutions consist of protein, ammonium acetate (BP of 117 ^{o}C), acetic acid (118^{o}C), the supercharger BC (> 238^{o}C), methanol (65^{o}C) and water (100^{o}C). During evaporation and fission, the volatile components methanol, ammonium acetate and water should readily evaporate, while the protein and BC should be preferentially enriched in the droplets. The presence of BC should also reduce evaporation rates of low volatility species owing to colligative properties (*i.e.* Raoult's Law). Any ammonium acetate remaining in the ESI droplet can limit the extent of protein ion charging owing to a buffering effect (*i.e.,* the optimal buffering capacity for

ammonium acetate is at pH 4.75)[47] hindering the lowering of the pH in the ESI droplets relative to droplets with lower ammonium acetate concentrations.[40] Alternatively, any residual ammonia/ammonium competes with proteins to acquire charge during emission from decomposing droplets. Charge is diverted to ammonia, when present.[48]

The extent of protein ion charging and unfolding was significantly higher when native protein solutions and denaturing supercharging solutions were mixed via θ-nanoESI compared to pre-mixing prior to nanoESI (**Figures 4, S5, S6**). In the shared Taylor cone mechanism of θ-nanoESI (**Figure 1c**), initial ionic droplets should consist of a ~1:1 mixture of the two solutions. That is, the composition of the ESI droplets should be comparable to the ESI droplets formed by single channel nanoESI of a 1:1 mixture of the two solutions. However, the extent of protein charging and unfolding obtained by θ-nanoESI is significantly higher than if the same solutions are pre-mixed prior to nanoESI (**Figures 4, S5, S6**). Therefore, the shared, single Taylor cone mechanism is inconsistent with these results.

Alternatively, in the two Taylor cone mechanism (**Figure 1c**), BC is not present in the same initial droplets as the ammonium acetate and thus cannot prevent evaporation of ammonium acetate early in the ESI process. Before droplet fusion, some solvent can evaporate, which should lower the concentration of ammonium acetate more than if BC was present in the droplet. Thus, after fusion of two droplets, the resulting droplet should have a reduced concentration of ammonium acetate than in the pre-mixed solutions. With a lower concentration of ammonium acetate, the protein can more readily unfold. This proposed model is more consistent with our observation that θ-nanoESI mixing results in protein ions with charge and conformations almost identical to those formed directly from denaturing supercharging solutions, and with significantly higher charging and more extensive protein unfolding than in-solution pre-mixing prior to nanoESI (**Figures 4, S5, S6**). These data also

indicate that highly charged protein ions formed via θ-nanoESI mixing can result from the near complete mixing of both solutions under these conditions.

CONCLUSIONS

Theta nanoelectrospray ionization can be used to form highly charged and unfolded protein ions directly from native solutions, with comparable charge and conformation to those formed from denaturing solutions. θ-nanoESI mixing of native and denaturing solutions can also result in the formation of protein ions that are more highly charged and unfolded than pre-mixing the same solutions prior to nanoESI. These results are consistent with the two Taylor cone mechanism[32] in which separate repulsive ion plumes emanate from each of the θ-nanoESI orifices as opposed to the shared Taylor cone mechanism.[27,29,30] These data are also consistent with charged droplets containing protein solution fusing with acidified droplets containing the supercharging additive 1,2-butylene carbonate, resulting in the formation of highly charged protein ions directly from a native solution.

θ-nanoESI of native protein solutions can result in the formation of ions in higher charge states than those formed directly from a denaturing solution,[28] which may now be explained by this mechanism. Droplet fusion is a high energy process that could potentially cause further protein unfolding. Droplet fusion should also result in larger droplets that may survive longer before the protein ion is formed. The formation of fully desolvated ions further into the ion source at lower pressures should reduce the extent of charge stripping that can occur by proton transfer reactions.[49] For example, protein ions in sufficiently high charge states such as those formed here from native solutions using θ-nanoESI mixing with a denaturing supercharging solution (such as the apo-myoglobin 31+ to 33+) can readily transfer a proton to N_2 and O_2 at room temperature and reduced pressure (low mTorr).[42]

The use of theta nanoelectrospray ionization has potential for improving protein sequencing experiments for biologically important proteins with unstable post-translational modifications (which may dissociate in denaturing solution), or that readily aggregate or decompose in denaturing conditions. Moreover, a clearer understanding of the mechanism of θ-nanoESI may potentially lead to the rational design of new supercharging additives to enable more efficient droplet fusion, and more accurate reaction kinetics from θ-nanoESI for studying highly reactive intermediates. It is also anticipated that the formation of highly charged and unfolded protein ions using θ-nanoESI emitters should be beneficial for many different types of isotopic (or reactive) labelling top-down MS/MS measurements to probe solution-phase protein structures.

SUPPORTING INFORMATION

Additional details on materials, additional mass spectra and arrival time distributions for protein ions, including control experiments.

ACKNOWLEDGEMENTS

This work was supported by funding from the Australian Research Council (FT200100798, DP190103298 to W.A.D), US National Institutes of Health (R01GM103479, S10OD018504 to J.A.L.), the US National Science Foundation (CHE1808492 to R.R.O.L and J.A.L) and the US Department of Energy (DE-FC02-02ER63421 to J.A.L.).

Present address:

†M.A.Z.: Australian Proteome Analysis Facility, 4 Wally's Walk, Macquarie University, Sydney 2109, Australia

REFERENCES

(1) Smith, L. M.; Agar, J. N.; Chamot-Rooke, J.; Danis, P. O.; Ge, Y.; Loo, J. A.; Paša-Tolić, L.; Tsybin, Y. O.; Kelleher, N. L. The Human Proteoform Project: Defining the

Human Proteome. *Sci. Adv.* **2021**, *7* (46).

(2) Fenn, J. B.; Mann, M.; Meng, C. K.; Wong, S. F.; Whitehouse, C. M. Electrospray Ionization for Mass Spectrometry of Large Biomolecules. *Science (80-.).* **1989**, *246* (4926), 64–71.

(3) Zenaidee, M. A.; Donald, W. A. Electron Capture Dissociation of Extremely Supercharged Protein Ions Formed by Electrospray Ionisation. *Anal. Methods* **2015**, *7* (17), 7132–7139.

(4) Zubarev, R. A.; Horn, D. M.; Fridriksson, E. K.; Kelleher, N. L.; Kruger, N. A.; Lewis, M. A.; Carpenter, B. K.; McLafferty, F. W. Electron Capture Dissociation for Structural Characterization of Multiply Charged Protein Cations. *Anal. Chem.* **2000**, *72* (3), 563–573.

(5) Syka, J. E. P.; Coon, J. J.; Schroeder, M. J.; Shabanowitz, J.; Hunt, D. F. Peptide and Protein Sequence Analysis by Electron Transfer Dissociation Mass Spectrometry. *Proc. Natl. Acad. Sci. U. S. A.* **2004**, *101* (26), 9528.

(6) Becher, S.; Wang, H.; Leeming, M. G.; Donald, W. A.; Heiles, S. Influence of Protein Ion Charge State on 213 Nm Top-down UVPD. *Analyst* **2021**, *146* (12), 3977–3987.

(7) Jarrold, M. F. Applications of Charge Detection Mass Spectrometry in Molecular Biology and Biotechnology. *Chem. Rev.* **2021**.

(8) Schnier, P. D.; Gross, D. S.; Williams, E. R. On the Maximum Charge State and Proton Transfer Reactivity of Peptide and Protein Ions Formed by Electrospray Ionization. *J. Am. Soc. Mass Spectrom.* **1995**, *6* (11), 1086–1097.

(9) Zhou, M.; Lantz, C.; Brown, K. A.; Ge, Y.; Paša-Tolić, L.; Loo, J. A.; Lermyte, F. Higher-Order Structural Characterisation of Native Proteins and Complexes by Top-down Mass Spectrometry. *Chem. Sci.* **2020**, *11* (48), 12918–12936.

(10) Bennett, J. L.; Nguyen, G. T. H.; Donald, W. A. Protein–Small Molecule Interactions in Native Mass Spectrometry. *Chem. Rev.* **2021**.

(11) Pan, J.; Han, J.; Borchers, C. H.; Konermann, L. Hydrogen/Deuterium Exchange Mass Spectrometry with Top-Down Electron Capture Dissociation for Characterizing Structural Transitions of a 17 KDa Protein. *J. Am. Chem. Soc.* **2009**, *131* (35), 12801–12808.

(12) Wang, G.; Abzalimov, R. R.; Bobst, C. E.; Kaltashov, I. A. Conformer-Specific Characterization of Nonnative Protein States Using Hydrogen Exchange and Top-down Mass Spectrometry. *Proc. Natl. Acad. Sci.* **2013**, *110* (50), 20087 LP – 20092.

(13) Pan, J.; Borchers, C. H. Top-down Mass Spectrometry and Hydrogen/Deuterium Exchange for Comprehensive Structural Characterization of Interferons: Implications for Biosimilars. *Proteomics* **2014**, *14* (10), 1249–1258.

(14) Pan, J.; Zhang, S.; Borchers, C. H. Protein Species-Specific Characterization of Conformational Change Induced by Multisite Phosphorylation. *J. Proteomics* **2016**, *134*, 138–143.

(15) Chen, J.; Cui, W.; Giblin, D.; Gross, M. L. New Protein Footprinting: Fast

Photochemical Iodination Combined with Top-Down and Bottom-Up Mass Spectrometry. *J. Am. Soc. Mass Spectrom.* **2012**, *23* (8), 1306–1318.

(16) Johnson, D. T.; Di Stefano, L. H.; Jones, L. M. Fast Photochemical Oxidation of Proteins (FPOP): A Powerful Mass Spectrometry Based Structural Proteomics Tool. *J. Biol. Chem.* **2019**, *294* (32), 11969–11979.

(17) Yang, Y.; Niu, C.; Bobst, C. E.; Kaltashov, I. A. Charge Manipulation Using Solution and Gas-Phase Chemistry to Facilitate Analysis of Highly Heterogeneous Protein Complexes in Native Mass Spectrometry. *Anal. Chem.* **2021**, *93* (7), 3337–3342.

(18) Lomeli, S. H.; Yin, S.; Ogorzalek Loo, R. R.; Loo, J. A. Increasing Charge While Preserving Noncovalent Protein Complexes for ESI-MS. *J. Am. Soc. Mass Spectrom.* **2009**, *20* (4), 593–596.

(19) Yin, S.; Loo, J. A. Top-down Mass Spectrometry of Supercharged Native Protein-Ligand Complexes. *Int. J. Mass Spectrom.* **2011**, *300* (2–3), 118–122.

(20) Sterling, H. J.; Williams, E. R. Origin of Supercharging in Electrospray Ionization of Noncovalent Complexes from Aqueous Solution. *J. Am. Soc. Mass Spectrom.* **2009**, *20* (10), 1933–1943.

(21) Sterling, H. J.; Cassou, C. A.; Trnka, M. J.; Burlingame, A. L.; Krantz, B. A.; Williams, E. R. The Role of Conformational Flexibility on Protein Supercharging in Native Electrospray Ionization. *Phys. Chem. Chem. Phys.* **2011**, *13* (41), 18288–18296.

(22) Sterling, H. J.; Daly, M. P.; Feld, G. K.; Thoren, K. L.; Kintzer, A. F.; Krantz, B. A.; Williams, E. R. Effects of Supercharging Reagents on Noncovalent Complex Structure in Electrospray Ionization from Aqueous Solutions. *J. Am. Soc. Mass Spectrom.* **2010**, *21* (10), 1762–1774.

(23) Lomeli, S. H.; Peng, I. X.; Yin, S.; Ogorzalek Loo, R. R.; Loo, J. A. New Reagents for Increasing ESI Multiple Charging of Proteins and Protein Complexes. *J. Am. Soc. Mass Spectrom.* **2010**, *21* (1), 127–131.

(24) Hogan Jr., C. J.; Ogorzalek Loo, R. R.; Loo, J. A.; de la Mora, J. F. Ion Mobility–Mass Spectrometry of Phosphorylase B Ions Generated with Supercharging Reagents but in Charge-Reducing Buffer. *Phys. Chem. Chem. Phys.* **2010**, *12* (41), 13476–13483.

(25) Sterling, H. J.; Cassou, C. A.; Susa, A. C.; Williams, E. R. Electrothermal Supercharging of Proteins in Native Electrospray Ionization. *Anal. Chem.* **2012**, *84* (8), 3795–3801.

(26) Yin, Z.; Huang, J.; Miao, H.; Hu, O.; Li, H. High-Pressure Electrospray Ionization Yields Supercharged Protein Complexes from Native Solutions While Preserving Noncovalent Interactions. *Anal. Chem.* **2020**, *92* (18), 12312–12321.

(27) Fisher, C. M.; Kharlamova, A.; McLuckey, S. A. Affecting Protein Charge State Distributions in Nano-Electrospray Ionization via in-Spray Solution Mixing Using Theta Capillaries. *Anal. Chem.* **2014**, *86* (9), 4581–4588.

(28) Wang, H.; Yong, G.; Brown, S. L.; Lee, H. E.; Zenaidee, M. A.; Supuran, C. T.; Donald, W. A. Supercharging Protein Ions in Native Mass Spectrometry Using Theta

Capillary Nanoelectrospray Ionization Mass Spectrometry and Cyclic Alkylcarbonates. *Anal. Chim. Acta* **2018**, *1003*, 1–9.

(29) Mortensen, D. N.; Williams, E. R. Theta-Glass Capillaries in Electrospray Ionization: Rapid Mixing and Short Droplet Lifetimes. *Anal. Chem.* **2014**, *86* (18), 9315–9321.

(30) Mark, L. P.; Gill, M. C.; Mahut, M.; Derrick, P. J. Dual Nano-Electrospray for Probing Solution Interactions and Fast Reactions of Complex Biomolecules. *Eur. J. Mass Spectrom.* **2012**, *18* (5), 439–446.

(31) Mortensen, D. N.; Williams, E. R. Ultrafast (1 Ms) Mixing and Fast Protein Folding in Nanodrops Monitored by Mass Spectrometry. *J. Am. Chem. Soc.* **2016**, *138* (10), 3453–3460.

(32) Jansson, E. T.; Lai, Y.-H.; Santiago, J. G.; Zare, R. N. Rapid Hydrogen–Deuterium Exchange in Liquid Droplets. *J. Am. Chem. Soc.* **2017**, *139* (20), 6851–6854.

(33) Kim, H. J.; Gallagher, E. S. Achieving Multiple Hydrogen/Deuterium Exchange Timepoints of Carbohydrate Hydroxyls Using Theta-Electrospray Emitters. *Analyst* **2020**, *145* (8), 3056–3063.

(34) Mortensen, D. N.; Williams, E. R. Microsecond and Nanosecond Polyproline II Helix Formation in Aqueous Nanodrops Measured by Mass Spectrometry. *Chem. Commun.* **2016**, *52* (82), 12218–12221.

(35) Radionova, A.; Greenwood, D. R.; Willmott, G. R.; Derrick, P. J. Dual Nano-Electrospray and Mixing in the Taylor Cone. *Mass Spectrom. Lett.* **2016**, *7* (1), 21–25.

(36) Bush, M. F.; Hall, Z.; Giles, K.; Hoyes, J.; Robinson, C. V; Ruotolo, B. T. Collision Cross Sections of Proteins and Their Complexes: A Calibration Framework and Database for Gas-Phase Structural Biology. *Anal. Chem.* **2010**, *82* (22), 9557–9565.

(37) Going, C. C.; Williams, E. R. Supercharging with M-Nitrobenzyl Alcohol and Propylene Carbonate: Forming Highly Charged Ions with Extended, Near-Linear Conformations. *Anal. Chem.* **2015**, *87* (7), 3973–3980.

(38) Shvartsburg, A. A.; Jarrold, M. F. An Exact Hard-Spheres Scattering Model for the Mobilities of Polyatomic Ions. *Chem. Phys. Lett.* **1996**, *261* (1), 86–91.

(39) Shelimov, K. B.; Jarrold, M. F. Conformations, Unfolding, and Refolding of Apomyoglobin in Vacuum: An Activation Barrier for Gas-Phase Protein Folding. *J. Am. Chem. Soc.* **1997**, *119* (13), 2987–2994.

(40) Zenaidee, M. A.; Donald, W. A. Extremely Supercharged Proteins in Mass Spectrometry: Profiling the PH of Electrospray Generated Droplets, Narrowing Charge State Distributions, and Increasing Ion Fragmentation. *Analyst* **2015**, *140* (6), 1894–1905.

(41) Teo, C. A.; Donald, W. A. Solution Additives for Supercharging Proteins beyond the Theoretical Maximum Proton-Transfer Limit in Electrospray Ionization Mass Spectrometry. *Anal. Chem.* **2014**, *86* (9), 4455–4462.

(42) Zenaidee, M. A.; Leeming, M. G.; Zhang, F.; Funston, T. T.; Donald, W. A. Highly Charged Protein Ions: The Strongest Organic Acids to Date. *Angew. Chemie Int. Ed.*

2017, *56* (29), 8522–8526.

(43) Loo, R. R. O.; Loo, J. A. Salt Bridge Rearrangement (SaBRe) Explains the Dissociation Behavior of Noncovalent Complexes. *J. Am. Soc. Mass Spectrom.* **2016**, *27* (6), 975–990.

(44) Kebarle, P.; Verkerk, U. H. Electrospray: From Ions in Solution to Ions in the Gas Phase, What We Know Now. *Mass Spectrom. Rev.* **2009**, *28* (6), 898–917.

(45) Cech, N. B.; Enke, C. G. Practical Implications of Some Recent Studies in Electrospray Ionization Fundamentals. *Mass Spectrom. Rev.* **2001**, *20* (6), 362–387.

(46) Fernandez de la Mora, J. Electrospray Ionization of Large Multiply Charged Species Proceeds via Dole's Charged Residue Mechanism. *Anal. Chim. Acta* **2000**, *406* (1), 93–104.

(47) Konermann, L. Addressing a Common Misconception: Ammonium Acetate as Neutral PH "Buffer" for Native Electrospray Mass Spectrometry. *J. Am. Soc. Mass Spectrom.* **2017**, *28* (9), 1827–1835.

(48) Ogorzalek Loo, R. R.; Lakshmanan, R.; Loo, J. A. What Protein Charging (and Supercharging) Reveal about the Mechanism of Electrospray Ionization. *J. Am. Soc. Mass Spectrom.* **2014**, *25* (10), 1675–1693.

(49) Xia, Z.; Williams, E. R. Effect of Droplet Lifetime on Where Ions Are Formed in Electrospray Ionization. *Analyst* **2019**, *144* (1), 237–248.

Supporting Information

On the mechanism of theta capillary nanoelectrospray ionization for the formation of highly charged protein ions directly from native solutions

Susannah L. Brown,[1] Muhammad A. Zenaidee,[2,†] Joseph A. Loo,[2] Rachel R. Ogorzalek Loo,[2] William A. Donald[1,*]

[1]School of Chemistry, University of New South Wales, Sydney 2052, Australia

[2]Department of Chemistry and Biochemistry, University of California Los Angeles, Los Angeles, California 90095, United States of America

[*]To whom correspondence should be addressed: w.donald@unsw.edu.au

Present address:

[†]M.A.Z.: Australian Proteome Analysis Facility, 4 Wally's Walk, Macquarie University, Sydney 2109, Australia

Table of Contents

Materials. Additional details on materials……..…S3

Supplementary Figure S1. Conventional nanoESI mass spectra of cytochrome *c*, apo-myoglobin, and carbonic anhydrase II with and without 1,2-butylene carbonate……S4

Supplementary Figure S2. Control native mass spectra and arrival time distributions of cytochrome *c*, apo-myoglobin, and carbonic anhydrase II formed from one channel of theta capillary….S10

Supplementary Figure S3. Mass spectra collected during optimisation of ESI spray voltage and tip-to-inlet distance……S5

Supplementary Figure S4. Mass spectra and arrival time distributions showing that tip orientation has minimal effect on protein charging and conformation…….S6

Supplementary Figure S5. Mass spectra and arrival time distributions of pre-mixed cytochrome *c* native and denaturing supercharging solutions formed from single channel nanoESI or one channel of a theta capillary…….S7

Supplementary Figure S6. Mass spectra and arrival time distributions of cytochrome *c* formed from theta nanoESI mixing, or a pre-mixed solution from one or two channels of a theta
capillary……S8

Supplementary Figure S7. Mass spectra and arrival time distributions of apo-myoglobin and carbonic anhydrase II ions formed by theta mixing or pre-mixing and nanoESI……S9

Materials: Cytochrome c from equine heart, apo-myoglobin from equine skeletal muscle and carbonic anhydrase II from bovine erythrocytes were purchased from Sigma Aldrich (St. Louis, MO). Carbonic anhydrase II was desalted before use using a 10 kDa cut-off centrifugal filter (Merck Millipore, Germany). 1,2-butylene carbonate was purchased from Tokyo Chemical Industry. Protein solutions were made in a 200 mM ammonium acetate solution unless otherwise stated.

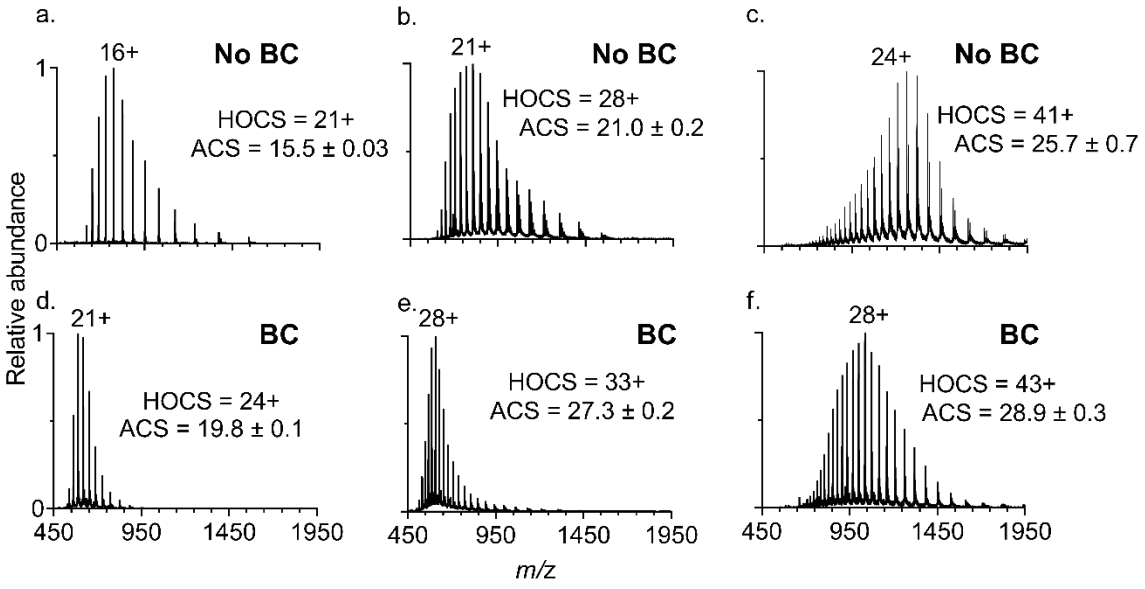

Figure S1. 1,2-butylene carbonate is used as an electrospray solution additive to enhance protein ion charging. Representative mass spectra for (a, d) cytochrome *c*, (b, e) apo-myoglobin and (c, f) carbonic anhydrase II formed from denaturing solutions with and without butylene carbonate (BC) by single channel nanoelectrospray ionization. Denaturing solutions contained 10 μM protein in 48.25/48.25/3.5/ water/methanol/acetic acid (%/% v/v). Solutions containing BC had the same composition as denaturing solutions and an additional 5% BC by volume. Highest observed charge state (HOCS) and average charge state (ACS) are indicated for each mass spectrum. The most abundant charge state is indicated on the spectra above the corresponding peaks.

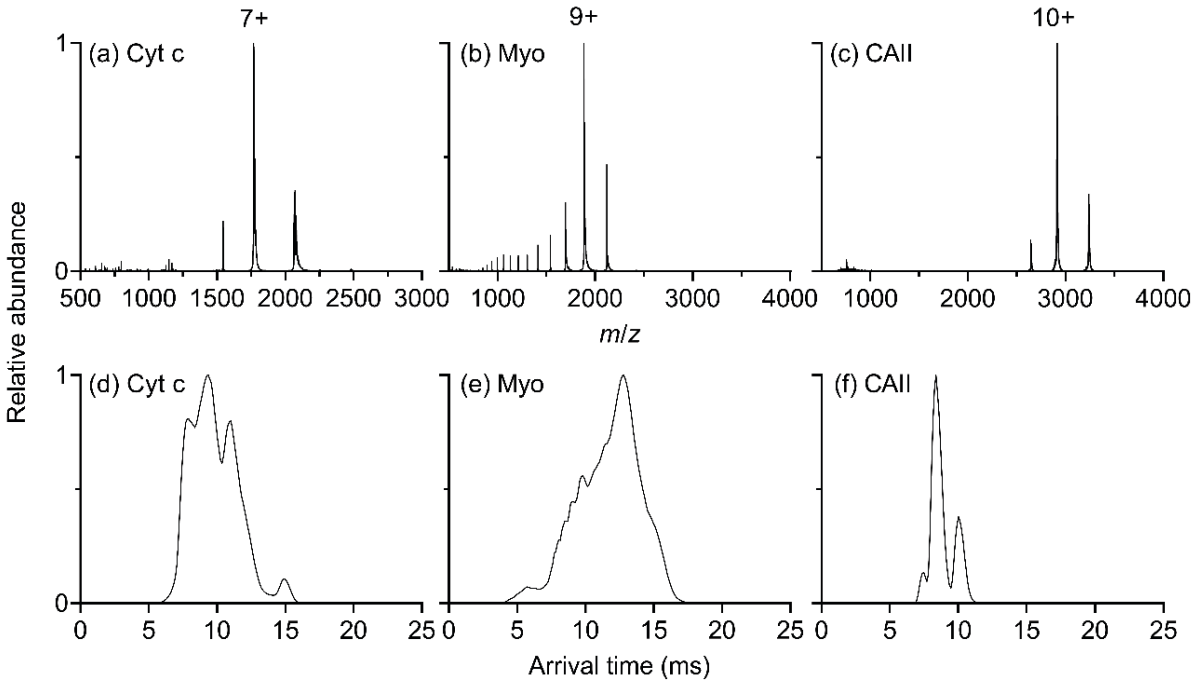

Figure S2. Control native nanoESI spectra formed from one channel of theta capillary. Representative mass spectra (a, b, c) and arrival time distributions (d, e, f) of cytochrome *c* (a, d), apo-myoglobin (b, d), and carbonic anhydrase II (c, f) formed by nanoESI of aqueous native solutions 200 mM ammonium acetate from one channel of a theta capillary. For apo-myoglobin, the high charge states that are formed in low abundance are typical of native mass spectra of this protein.[1] Without the heme group, the protein structures are destabilized.

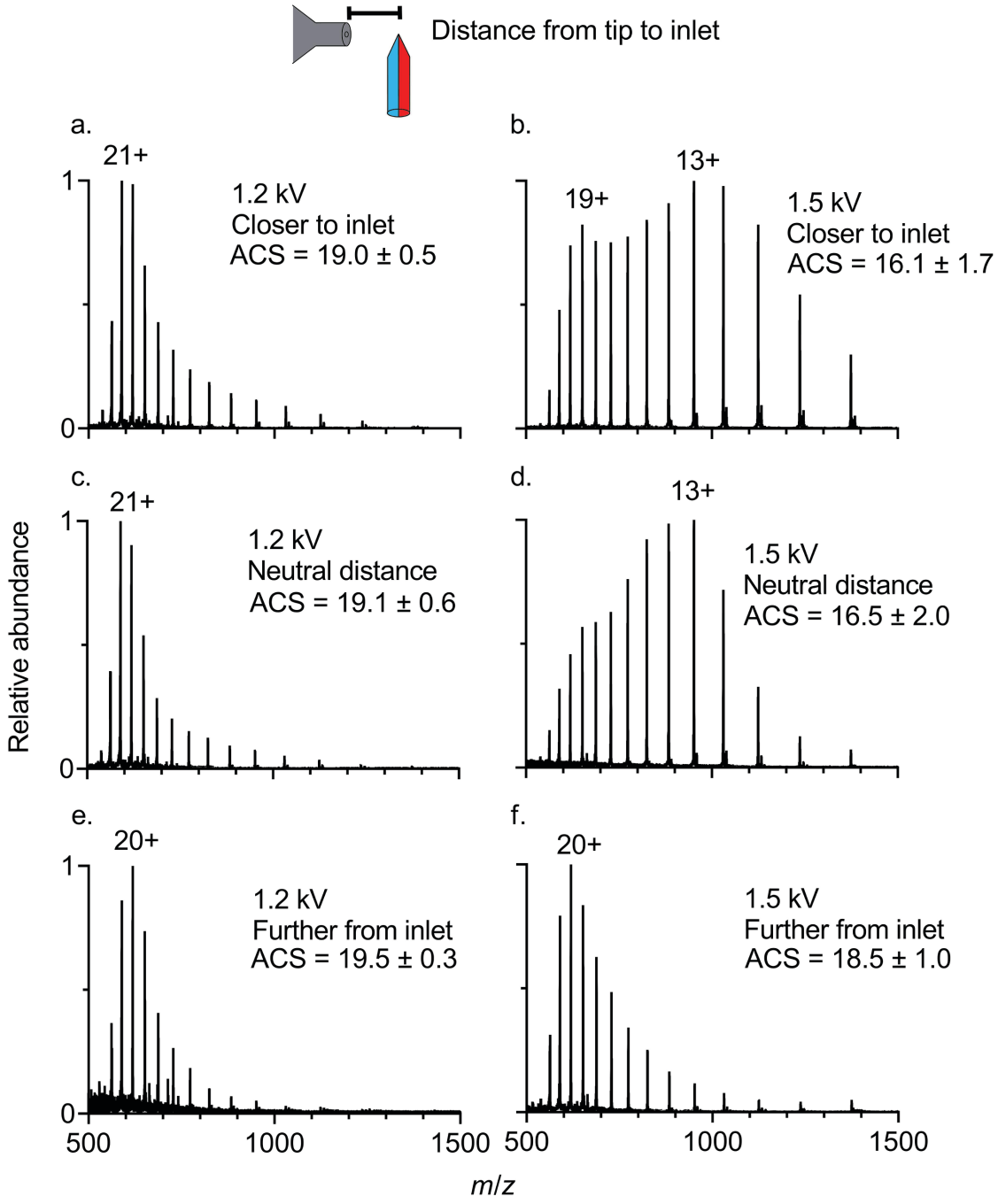

Figure S3. **Optimisation of ESI spray voltage and tip-to-inlet distance.** Panels a-f display mass spectra collected during optimisation of spray voltage and distance from tip to MS inlet.

ESI spray voltage 1.2 kV with tip at neutral distance relative to the MS inlet were deemed the optimum conditions for charging and signal.

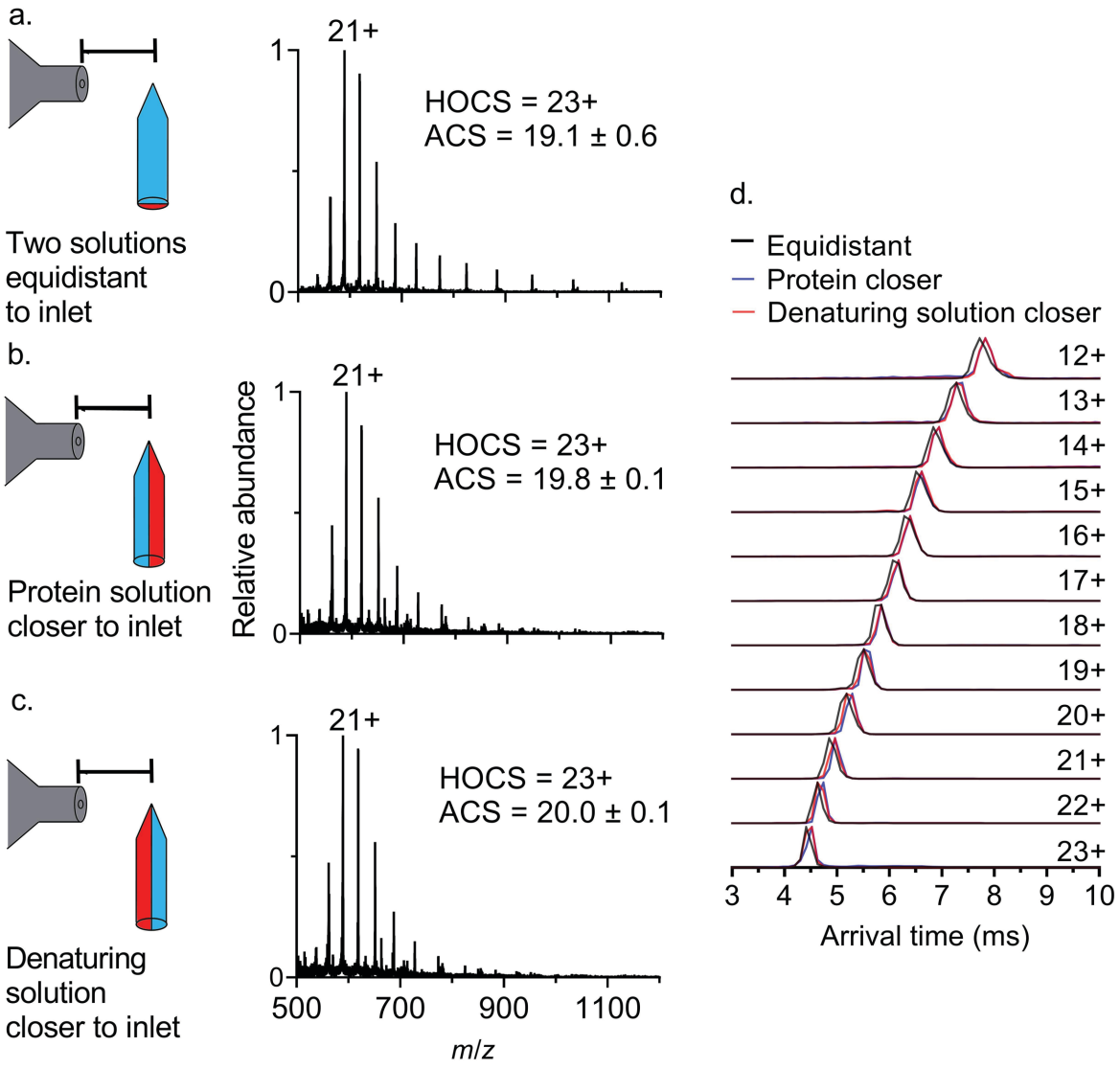

Figure S4. Orientation of θ-nanoESI tip relative to the inlet of the MS has minimal effect of protein ion charging and conformation. Effect on charge state distributions of cytochrome *c* formed from a theta capillary (Channel 1: 10 μM cytochrome *c* solution in 200 mM ammonium acetate buffer (pH ~7), Channel 2: 41.5/41.5/10/7 water/methanol/1,2-butylene carbonate/acetic acid(%/% v/v)) of different orientations of the theta tip relative to the mass spectrometer inlet. Diagrams in (a-c) show the orientation of the tip where the blue represents native protein solution and red the denaturing-supercharging solution. Highest observed charge state (HOCS), average charge state (ACS), and most abundant charge state are indicated on the spectra. (d) TWIMS arrival time distributions of individual charge states when formed from each of the three theta tip orientations.

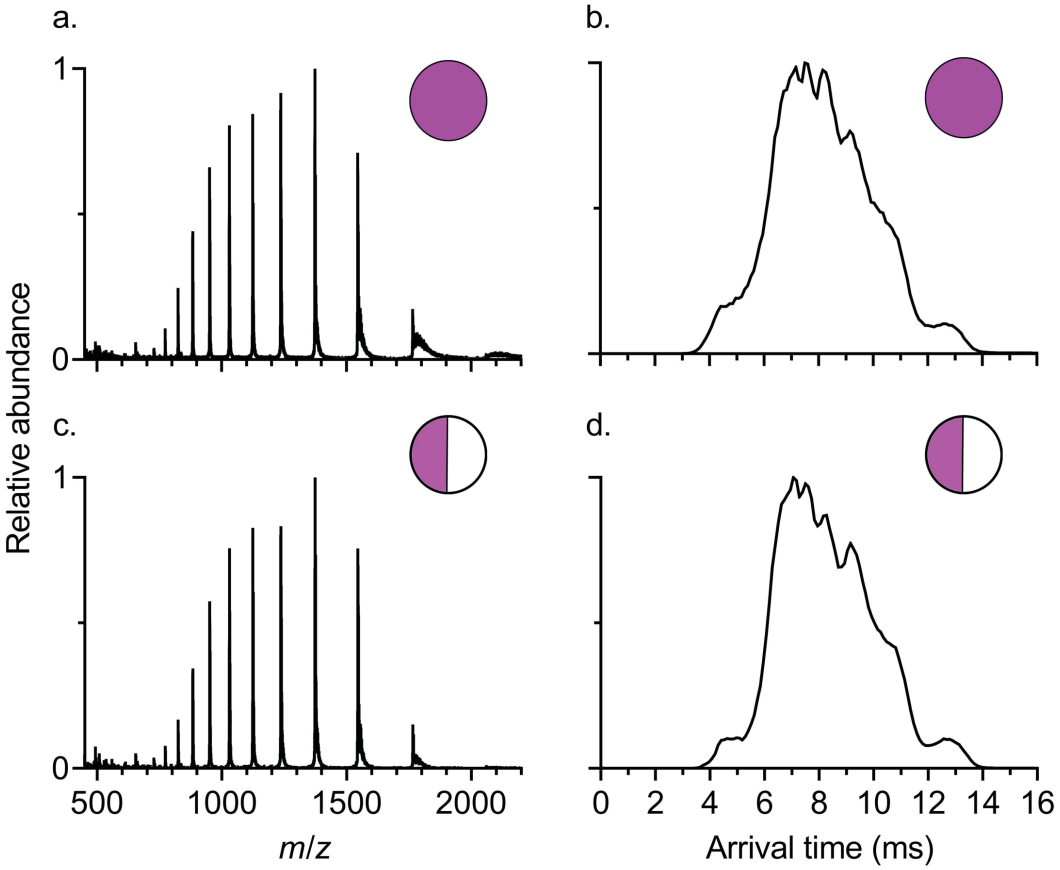

Figure S5. Theta tip geometry does not affect protein ion charging and conformation compared to single channel nanoESI. (a, c) Mass spectra and (b, d) arrival time distributions for cytochrome *c* ions formed from 1:1 (volume:volume) pre-mixed solution of 10 μM cytochrome *c* solution in 200 mM ammonium acetate (pH ~7) and 41.5/41.5/10/7 water/methanol/1,2-butylene carbonate/acetic acid (%/% v/v). The two solutions were mixed just prior to nanoESI. The solution was electrosprayed from either a (a-b) single channel capillary or (c-d) one channel of a theta capillary. Spectra are nearly identical in both cases ruling out any structural effects caused by the theta capillary itself.

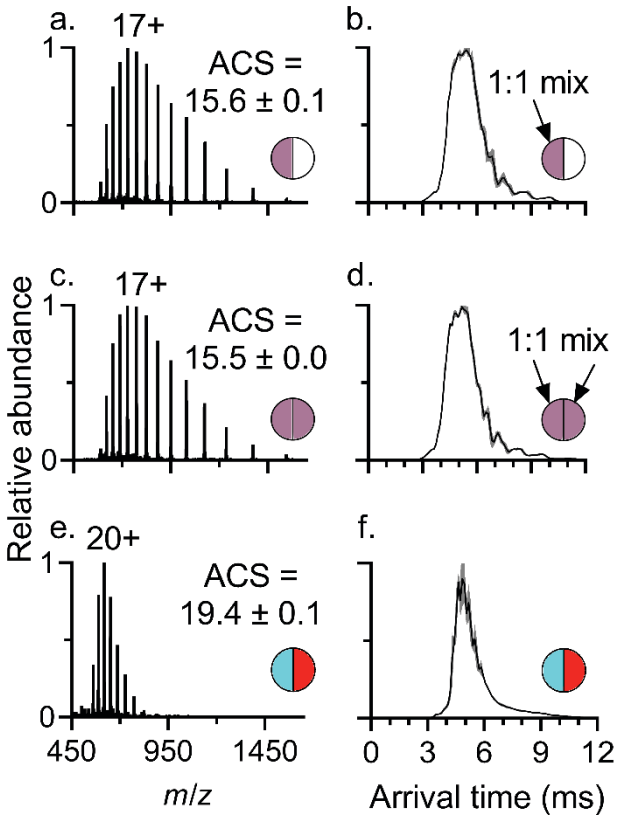

Figure S6. Theta nanoESI mixing of native protein solutions and denaturing, supercharging solutions results in significantly higher charging compared to in-solution pre-mixing and is not a result of theta emitter tip geometry. Representative (a, c, e) mass spectra and (b, d, f) TWIMS arrival time distributions of cytochrome *c* ions formed from either (a-d) in-solution or (f-g) theta nanoESI mixing of a 10 μM cytochrome *c* solution in 200 mM ammonium acetate buffer (pH ~7) with a solution of 41.5/41.5/10/7 water/methanol/1,2-butylene carbonate/acetic acid (%/% v/v). For in-solution pre-mixing, the solution was incubated overnight to reach equilibrium. The equilibrated mixture was loaded into either (a-b) one channel of a theta capillary (purple semicircle), or (c-d) both channels of a theta capillary (two purple semi-circles). Half-blue half-red circle indicates a theta capillary with one side containing native protein solution (blue) and the other side the denaturing solution (red). Most abundant charge state and average charge states (ACS) are labelled. Shaded areas on arrival time distributions indicate standard deviations from triplicate measurements.

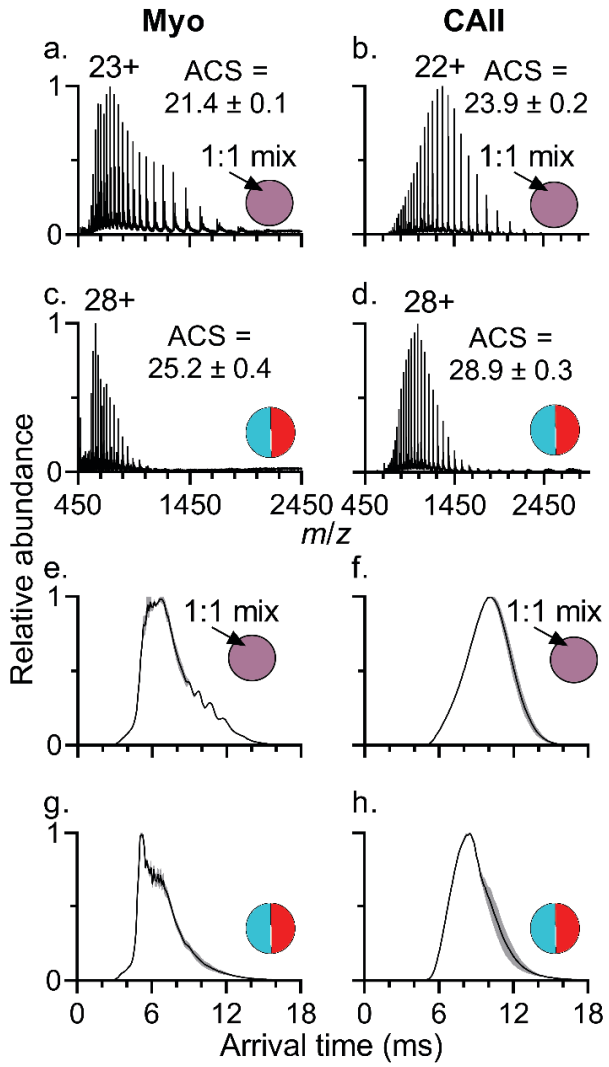

Figure S7. θ-nanoESI mixing of native solutions of larger proteins and denaturing, supercharging solutions results in higher protein charge states than if solutions are mixed prior to nanoESI. Representative (a-d) mass spectra and (e-h) arrival time distributions for (a, c, e, g) apo-myoglobin and (b, d, f, h) carbonic anhydrase II ions formed from either (a-b, e-f) in-solution or (c-d, g-h) theta capillary mixing of a 10 μM protein solution in 200 mM ammonium acetate buffer (~pH 7) with a solution of 41.5/41.5/10/7 water/methanol/1,2-butylene carbonate/acetic acid (%/% v/v). Average and most abundant charge states are labelled. Shaded areas on arrival time distributions indicate standard deviations from triplicate measurements, with the exception of (e) which was done in duplicate.

References

(1) Cammarata, M. B.; Brodbelt, J. S. Structural Characterization of Holo- and Apo-Myoglobin in the Gas Phase by Ultraviolet Photodissociation Mass Spectrometry. *Chem. Sci.* **2015**, *6* (2), 1324–1333.